*Desalination and Water Treatment*
www.deswater.com
doi: 10.1080/19443994.2014.972985

57 (2016) 747–753
January

Taylor & Francis
Taylor & Francis Group

# Removal of methyl orange from aqueous solution by EA/Triton-X100/EG/water green nanoemulsions

Faiyaz Shakeel[a,*], Nazrul Haq[a], Fars K. Alanazi[a,b], Ibrahim A. Alsarra[a,b]

[a]*Center of Excellence in Biotechnology Research, College of Science, King Saud University, P.O. Box 2460, Riyadh 11451, Saudi Arabia, email: faiyazs@fastmail.fm (F. Shakeel)*
[b]*Department of Pharmaceutics, College of Pharmacy, King Saud University, P.O. Box 2457, Riyadh 11451, Saudi Arabia*

Received 3 April 2014; Accepted 25 September 2014

---

## ABSTRACT

In the present study, attempts were made to develop green nanoemulsions for the removal of methyl orange (MO) from its bulk aqueous solution. Different nanoemulsions were prepared by low-energy emulsification method using ethyl acetate (EA) (oil phase), Triton-X100 (surfactant), ethylene glycol (EG) (cosurfactant), and deionized water (aqueous phase). Prepared nanoemulsions were characterized for thermodynamic stability, self-nanoemulsification efficiency, droplet size, polydispersity, viscosity, refractive index, and transmittance. Adsorption studies were carried out at different contact time (10, 15, and 20 min) by mixing small amounts of nanoemulsions with relatively large amounts of MO aqueous solution. The influence of contact time and EA concentration on droplet size, viscosity, and % MO removal was also studied. The droplet size, viscosity, and % MO removal efficiency were significantly influenced by EA concentration. Based on the lowest droplet size (18.6 nm), lowest viscosity (16.2 cp), and highest % MO removal efficiency (81.6%), the nanoemulsion $G_1$ (containing 5% w/w of EA, 23.3% w/w of Triton-X100, 11.7% w/w of EG, and 60% w/w of water) was optimized as the best formulation for the removal of MO from aqueous solution after 20 min of contact time. These results indicated that the prepared nanoemulsions could be used as potential liquid-based adsorbents for the removal of MO from aqueous solution.

*Keywords:* Adsorption; Ethyl acetate; Green nanoemulsions; Methyl orange; Droplet size

---

## 1. Introduction

Considerable amount of wastewater effluents contain synthetic colors/dyes have been generated from several commercial industries such as leather, textile, paper, printing, pharmaceutical, food, dyestuff, plastic, and so on [1–3]. These synthetic colors/dyes are difficult to biodegrade and present significant toxicity such as carcinogenicity and mutagenicity [1,4–6]. Removal of these colors/dyes from water/wastewater effluent is very important because they influenced the water quality significantly and even small amount of these colors/dyes is highly visible and undesirable [1,7]. Methyl orange (MO) is a well-known anionic acidic-dye which is widely used in paper, printing, textile, food, and pharmaceutical industries as well as in research laboratories [7,8]. For the removal of these dye materials from water/wastewater effluents, various methods including physical, chemical, and biological methods have been reported in literature [6,9–11]. Solid–liquid adsorption is frequently used method for

---

*Corresponding author.

wastewater treatment among all these methods [3,12,13]. Nevertheless, each method of dye removal had its own limitations and the adsorption efficiency of any method is not very high to achieve desired goals [6,14]. Hence, it is of great significance to develop a simple, cheaper, environmentally benign, and cost effective technique for the removal of these toxic dyes from water. Recently, more attention has been paid toward the use of nanoscale-based systems for the removal of these synthetic dyes from industrial wastewater effluents or aqueous solutions [6,15,16]. Nanoemulsions are thermodynamically stable nanoscale colloidal carriers which composed of oil, surfactant, cosurfactant, and water with droplet size usually in the range of 10–100 nm [17–19]. These liquid-based adsorbents (nanoemulsions) offered several advantages such as thermodynamic stability, excellent extraction capacity, ease of preparation, spontaneous adsorption, low preparation cost, less contact time for dye removal, and avoidance of use of organic solvents over other methods used for dye removal [6,17–19]. These liquid-based systems such as nanoemulsions and microemulsions have been investigated for the removal of various toxic dyes (methylene blue, xylenol orange, Eriochrome black T, and Congo red), micropollutant (indomethacin), and toxic metals (chromium and thorium) [6,20–25]. To the best of our knowledge, nanoemulsions have never been investigated for the removal of MO from aqueous solution or wastewater effluents in literature. Therefore, attempts were made to develop nanoemulsions for the removal of anionic acidic-dye MO from its bulk aqueous solution via liquid–liquid adsorption. Nanoemulsions were developed by low energy emulsification method (aqueous phase titration method). The nanoemulsion system used in this study is called as green nanoemulsion because all the components of nanoemulsion such as ethyl acetate (EA) (oil phase), octylphenoxypolyethoxyethanol (Triton-X100) (surfactant), ethylene glycol (EG) (cosurfactant), and deionized water (aqueous phase) are green solvents/excipients. Low-energy emulsification methods include two methods for nanoemulsion preparation namely aqueous phase titration method and phase inversion temperature (PIT) method. In PIT method, nanoemulsions are prepared either by changing the nanoemulsion compositions at constant temperature or changing the temperature at constant composition [26,27]. However, in aqueous phase titration method, nanoemulsions are prepared by titrating the mixture of oil and surfactants with aqueous phase at constant temperature [27]. All these materials are safe and considered as eco-friendly/environmentally benign.

## 2. Materials and methods

### 2.1. Materials

EA (Winlab Laboratory, Leicestershire, UK), Triton-X100 (BDH Laboratory, Liverpool, UK), EG (Winlab Laboratory, Leicestershire, UK), and MO (Sigma Aldrich, St. Louis, MO) were used in present study. Deionized water was obtained from ELGA water purification system (Wycombe, UK).

### 2.2. Development of EA/Triton-X100/EG/water nanoemulsions

For the development of EA/Triton-X100/EG/water nanoemulsions, EA, Triton-X100, EG, and deionized water were used as oil phase, surfactant, cosurfactant, and aqueous phase, respectively. Oil-in-water (o/w) type EA/Triton-X100/EG/water nanoemulsions were developed by low-energy emulsification method as reported in our previous articles [6,17]. These nanoemulsions were prepared via construction of pseudoternary phase diagrams by low-energy emulsification method [21]. Briefly, surfactant and cosurfactant were mixed at mass ratios of 3:1 to 1:0. Oil phase and specific combination of surfactant and cosurfactant ($S_{\mathrm{mix}}$) were then mixed in mass ratios of 1:9 to 9:1. Pseudoternary phase diagrams were constructed by aqueous phase titration method (data not shown) [21]. Highest nanoemulsion zones were exposed by $S_{\mathrm{mix}}$ ratio of 2:1. Therefore, various nanoemulsions were prepared from 2:1 $S_{\mathrm{mix}}$ ratio (Table 1).

### 2.3. Physicochemical characterization of EA/Triton-X100/EG/water nanoemulsions

Developed EA/Triton-X100/EG/water nanoemulsions were characterized for thermodynamic stability, self-nanoemulsification efficiency, droplet size distribution, polydispersity index (PI), viscosity, refractive index (RI), and percentage of transmittance (% $T$). EA/Triton-X100/EG/water nanoemulsions ($G_1$–$G_6$) were subjected to various thermodynamic stress tests such as centrifugation (at 5,000 rpm for 30 min), heating and cooling cycles (3 cycles between 25 and 45°C for 48 h), and freeze-pump-thaw cycles (3 cycles between −21 and 25°C). Thermodynamically stable nanoemulsions were selected further for self-nanoemulsification efficiency test [17,18].

The self-nanoemulsification performance of EA/Triton-X100/EG/water nanoemulsions ($G_1$–G6) was assessed in water [6,17]. Briefly, 1 g of each nanoemulsion was gently mixed with 200 ml of water at room temperature (25 ± 0.5°C). The self-nanoemulsifying

Table 1
Composition of EA/Triton-X100/EG/water nanoemulsions

| Code | EA (% w/w) | TX-100 (% w/w) | EG (% w/w) | Water (% w/w) | $S_{mix}$ ratio |
|---|---|---|---|---|---|
| $G_1$ | 5.0 | 23.3 | 11.7 | 60.0 | 2:1 |
| $G_2$ | 10.0 | 23.3 | 11.7 | 55.0 | 2:1 |
| $G_3$ | 15.0 | 23.3 | 11.7 | 50.0 | 2:1 |
| $G_4$ | 20.0 | 23.3 | 11.7 | 45.0 | 2:1 |
| $G_5$ | 25.0 | 23.3 | 11.7 | 40.0 | 2:1 |
| $G_6$ | 30.0 | 23.3 | 11.7 | 35.0 | 2:1 |

Note: Ethyl acetate (EA), Triton-X100 (TX-100), ethylene glycol (EG), ratio of surfactant to cosurfactant ($S_{mix}$).

performance of each nanoemulsion was assessed visually using A-E grading systems as reported previously [6,18,19].

The droplet size distribution and PI of EA/Triton-X100/EG/water nanoemulsions ($G_1$–$G_6$) were determined using Brookhaven particle size analyzer (Brookhaven Instrument Corporation, USA) as described previously [18]. Each experiment was carried out in triplicates.

The viscosity of EA/Triton-X100/EG/water nanoemulsions ($G_1$–$G_6$) was recorded using Brookfield viscometer (Brookfield Engineering Laboratories, Inc, Middleboro, MA) [17]. However, the RI of EA/Triton-X100/EG/water nanoemulsions ($G_1$–$G_6$) was recorded using Abbes type refractometer (Precision Standard Testing Equipment Corporation, Germany) as reported in literature [6,17]. Each experiment was carried out in triplicates.

% *T* of EA/Triton-X100/EG/water nanoemulsions ($G_1$–$G_6$) was recorded spectrophotometerically (SPUV-19, Dingelstadt, Germany) at 550 nm according to the previous literature [19]. Each experiment was carried out in triplicates.

### 2.4. Preparation of MO stock solution and calibration curve

The stock solution (200 ppm) of MO was prepared by dissolving the required amount of MO dye in deionized water. From this stock solution, serial dilutions were prepared to obtain concentration in the range of 1–25 ppm. The absorbance of each concentration of MO was recorded spectrophotometrically (SP-1900, Axiom, Germany) at 464 nm [7]. The calibration curve was plotted between the concentration and absorbance of MO. The proposed analytical method was observed linear in the concentration range of 1–25 ppm with correlation coefficient of 1.000.

### 2.5. Adsorption experiments for MO removal from aqueous solution

Adsorption experiments were performed by mixing small amount (1 ml) of EA/Triton-X100/EG/water nanoemulsions ($G_1$–$G_6$) with relatively large amount (10 ml) of MO solution (200 ppm) in 25 ml capacity conical flasks in triplicates. Each nanoemulsion-treated MO solution was kept in laboratory bench at 25°C. At different time intervals (10, 15, and 20 min), each nanoemulsion-treated MO solution was subjected to destabilization via freeze thaw and heating. Freeze thawing was performed at −21°C for 3 h. However, the heating was performed by exposing the samples in hot air oven at 60°C for 2 h. Each nanoemulsion-treated MO solution was diluted suitably with methanol in order to avoid interference peaks of oils during analysis [20]. The residual concentration of MO was determined in supernatant of each nanoemulsion-treated dye solution at 464 nm [7]. The amount of MO adsorbed on to the surface of different EA/Triton-X100/EG/water nanoemulsions ($G_1$–$G_6$) at time *t* ($q_t$ in μg/g) was calculated using Eq. (1):

$$q_t = \frac{C_0 - C_t}{m} \times V \qquad (1)$$

However, % MO removal efficiency (%*E*) of EA/Triton-X100/EG/water nanoemulsions ($G_1$–$G_6$) was calculated using Eq. (2):

$$\% E = \frac{C_0 - C_t}{C_0} \times 100 \qquad (2)$$

where $C_0$ and $C_t$ are the initial concentration of MO (ppm) and MO concentration (ppm) at time *t*, respectively. However, *V* and *m* represent the volume of solution (ml) and mass of nanoemulsion (g), respectively [3].

## 3. Results and discussion

### 3.1. Development of EA/Triton-X100/EG/water nanoemulsions

The primary criteria for selection of various components of nanoemulsion, such as oil, surfactant, and cosurfactant, was their safety and green nature as the purpose of this study was to develop green nanoemulsions. Various EA/Triton-X100/EG/water nanoemulsions were developed by low-energy emulsification method in order to get optimum composition of oil, surfactant, cosurfactant, and water for removal of MO from its aqueous solution. $S_{\text{mix}}$ ratio of 2:1 was selected for preparation of EA/Triton-X100/EG/water nanoemulsions as it showed the highest nanoemulsion zones in pseudo-ternary phase diagrams in our previous article [21]. For the development of EA/Triton-X100/EG/water nanoemulsions, the concentration of EA was varied from 5 to 30% w/w and the concentration of $S_{\text{mix}}$ was kept constant at 35% w/w. The composition of these nanoemulsions is listed in Table 1.

### 3.2. Physicochemical characterization of EA/Triton-X100/EG/water nanoemulsions

The main objective of thermodynamic stability tests was to remove any unstable/metastable composition of EA/Triton-X100/EG/water nanoemulsions. The results of thermodynamic stability tests are listed in Table 2. Developed EA/Triton-X100/EG/water nanoemulsions ($G_1$–$G_6$) were found to be stable at all steps of thermodynamic stability tests (Table 2). Thermodynamically stable EA/Triton-X100/EG/water nanoemulsions ($G_1$–$G_6$) were further investigated for self-nanoemulsification performance using water as a dispersion media. The results of self-nanoemulsifying performance are also listed in Table 2. It was observed that most of the developed EA/Triton-X100/EG/water nanoemulsions (except $G_6$) passed this test with grade A (Table 2) which is an excellent grade for self-dispersible nanoemulsions.

The droplet size of EA/Triton-X100/EG/water nanoemulsions ($G_1$–$G_6$) was observed in the range of 18.6–62.5 nm (Table 3). The droplet size of EA/Triton-X100/EG/water nanoemulsions ($G_1$–$G_6$) was found to be reduced significantly by decreasing the concentration of EA (oil phase) in the formulations (Table 3) which indicated that the concentration of EA had significant impact on droplet size of EA/Triton-X100/EG/water nanoemulsions. Overall, the droplet size was observed the lowest in nanoemulsion $G_1$ (18.6 nm). However, the highest one was observed in nanoemulsion $G_6$ (62.5 nm). The lowest and the highest droplet size in formulations $G_1$ and $G_6$ were probably due to the presence of the lowest and the highest concentrations of EA (oil phase) in $G_1$ and $G_6$, respectively.

The PI of EA/Triton-X100/EG/water nanoemulsions ($G_1$–$G_6$) was observed in the range of 0.128–0.248, indicating the uniformity in droplet size distribution in all nanoemulsions (Table 3). The PI was found to be the lowest in nanoemulsion $G_1$ (0.128) and the highest in $G_6$ (0.248). The RI of EA/Triton-X100/EG/water nanoemulsions ($G_1$–$G_6$) was observed in the range of 1.334–1.342 (Table 3). The values of RIs were very close to RI of water (1.33) in all nanoemulsions which indicated the transparent nature and o/w type behavior of all nanoemulsions. The viscosity of EA/Triton-X100/EG/water nanoemulsions ($G_1$–$G_6$) was observed in the range of 16.2–58.4 cp (Table 3). The lower viscosities in all nanoemulsions indicated the free flowing nature of all these formulations. The lowest and the highest viscosities were observed in nanoemulsions $G_1$ (16.2 cp) and $G_6$ (58.4 cp), respectively. The % $T$ of EA/Triton-X100/EG/water nanoemulsions ($G_1$–$G_6$) was observed in the range of 98.0–98.6% (Table 3) which also indicated the transparent nature

Table 2
Results of thermodynamic stability and self-nanoemulsification tests of EA/Triton-X100/EG/water nanoemulsions ($G_1$–$G_6$)

| | | Thermodynamic stability tests | | |
|---|---|---|---|---|
| Code | Self-nanoemulsification test grade | Cent. | H&T | FPT |
| $G_1$ | A | √ | √ | √ |
| $G_2$ | A | √ | √ | √ |
| $G_3$ | A | √ | √ | √ |
| $G_4$ | A | √ | √ | √ |
| $G_5$ | A | √ | √ | √ |
| $G_6$ | B | √ | √ | √ |

Note: √(Passed the respective test), cent. (centrifugation), H&T (heating and cooling cycles), FPT (freeze-pump-thaw cycles).

Table 3
Physicochemical characterization of EA/Triton-X100/EG/water nanoemulsions ($G_1$–$G_6$) ($n$ = 3)

| Code | Characterization parameters | | | | |
|---|---|---|---|---|---|
| | $\Delta dm^{\#}$ ± SD (nm) | PI* | $\eta$ ± SD (cp) | RI ± SD | % $T$ ± SD |
| $G_1$ | 18.6 ± 1.9 | 0.128 | 16.2 ± 1.8 | 1.334 ± 0.011 | 98.6 ± 0.3 |
| $G_2$ | 24.6 ± 2.8 | 0.133 | 22.3 ± 3.7 | 1.335 ± 0.010 | 98.5 ± 0.4 |
| $G_3$ | 31.6 ± 3.0 | 0.139 | 30.3 ± 3.9 | 1.336 ± 0.010 | 98.4 ± 0.2 |
| $G_4$ | 36.8 ± 4.1 | 0.192 | 34.2 ± 4.1 | 1.337 ± 0.012 | 98.3 ± 0.2 |
| $G_5$ | 41.3 ± 4.8 | 0.228 | 39.1 ± 4.6 | 1.341 ± 0.017 | 98.2 ± 0.3 |
| $G_6$ | 62.5 ± 6.7 | 0.248 | 58.4 ± 5.9 | 1.342 ± 0.018 | 98.0 ± 0.3 |

[#]Mean droplet diameter ($\Delta dm$).

*Polydispersity index (PI).

Note: Viscosity mean ($\eta$), % $T$ (% transmittance), standard deviation (SD).

of all formulations. The highest and the lowest % $T$ were also observed in nanoemulsions $G_1$ (98.6%) and $G_6$ (98.0%), respectively.

### 3.3. Adsorption studies for removal of MO from aqueous solution

After proper development and physicochemical characterization of EA/Triton-X100/EG/water nanoemulsions ($G_1$–$G_6$), the efficiency of these formulations was investigated in the removal of MO from its bulk aqueous solution. The MO removal efficiencies of EA/Triton-X100/EG/water nanoemulsions ($G_1$–$G_6$) were determined at different contact time (10, 15, and 20 min). The results of % adsorption of MO onto the surface of EA/Triton-X100/EG/water nanoemulsions ($G_1$–$G_6$) at different contact time are listed in Table 4. The % MO removal efficiencies of EA/Triton-X100/EG/water nanoemulsions ($G_1$–$G_6$) were observed in the range of 32.6–81.6% (Table 4). It was observed that contact time had negligible impact on % MO removal from aqueous solution because no significant changes were observed in % MO removal with contact time (Table 4). Nanoemulsion $G_1$ showed highest % MO removal (81.6%) after 20 min as compared to other nanoemulsions. However, nanoemulsion $G_6$ showed the lowest % MO removal. The influence of EA concentration on % MO removal after 20 min of contact time is presented in Fig. 1. From Fig. 1, it was observed that when the concentration of EA was increased from 5 to 30% w/w, the % removal of MO decreased significantly (Fig. 1). These results indicated that the concentration of EA (oil phase) had greater impact on % MO removal efficiencies of EA/Triton-X100/EG/water nanoemulsions ($G_1$–$G_6$). These results were in agreement with recently published data of Congo red, xylenol orange, and methylene blue [6,20,22]. The droplet size and viscosity of EA/Triton-X100/EG/water nanoemulsions ($G_1$–$G_6$) were also cor-

Table 4
Percentage (%) of MO adsorption onto the surface of EA/Triton-X100/EG/water nanoemulsions ($G_1$–$G_6$) at different contact time ($n$ = 3)

| | % MO adsorption at different contact time (min) | | |
|---|---|---|---|
| Code | 10 | 15 | 20 |
| $G_1$ | 81.3 ± 0.6 | 81.5 ± 0.8 | 81.6 ± 0.9 |
| $G_2$ | 72.4 ± 0.4 | 72.7 ± 0.5 | 72.8 ± 0.3 |
| $G_3$ | 64.2 ± 0.3 | 64.4 ± 0.2 | 64.6 ± 0.4 |
| $G_4$ | 56.3 ± 0.6 | 56.5 ± 0.7 | 56.7 ± 0.8 |
| $G_5$ | 48.5 ± 0.7 | 48.8 ± 0.8 | 48.9 ± 0.9 |
| $G_6$ | 32.6 ± 0.2 | 32.8 ± 0.4 | 32.9 ± 0.3 |

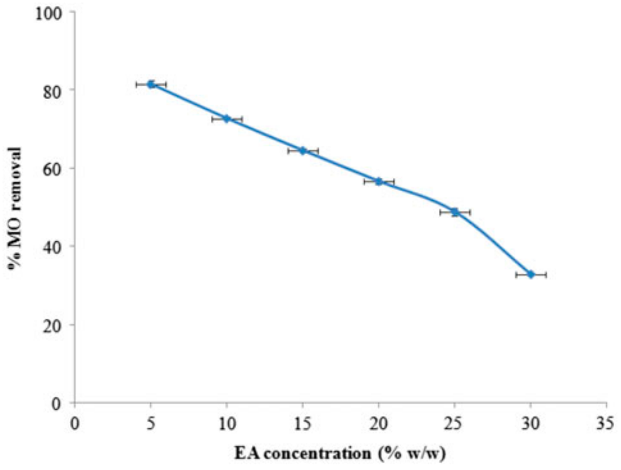

Fig. 1. Impact of EA concentration on % MO removal at 35% w/w of $S_{\text{mix}}$ concentrations after 20 min of contact time ($n$ = 3).

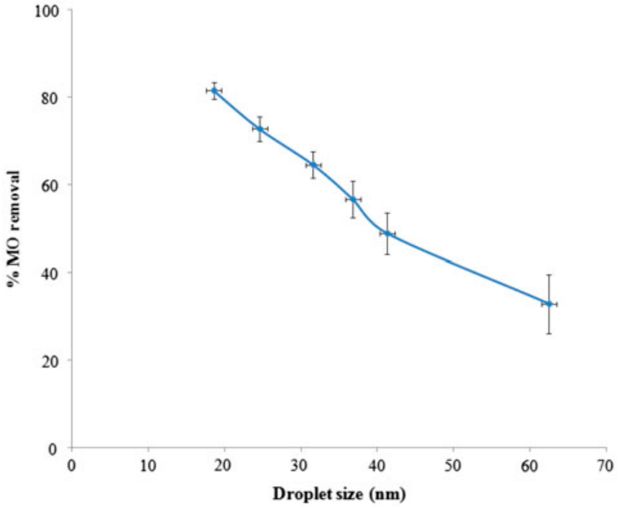

Fig. 2. Impact of droplet size of EA/Triton-X100/EG/water nanoemulsions on % MO removal ($n = 3$).

related with % MO removal from its aqueous solution. The influence of droplet size and viscosity on MO removal is presented in Figs. 2 and 3, respectively. The % MO removal was found to be increased significantly with decrease in droplet size and viscosity of EA/Triton-X100/EG/water nanoemulsions ($G_1$–$G_6$) as shown in Figs. 2 and 3, respectively. Overall, the highest % MO removal efficiency was shown by nanoemulsion $G_1$ (81.6% after 10 min). However, the lowest one was shown by nanoemulsion $G_6$ (32.6% after 10 min). The highest and the lowest MO removal efficiencies in nanoemulsions $G_1$ and $G_6$ were possibly due to the lowest (18.6 nm) and the highest (62.5 nm) droplet size of $G_1$ and $G_6$, respectively. Recently, the influence of droplet size and viscosity of nanoemulsions was also investigated in the removal of micropollutant indomethacin and toxic dye Congo red [22,25]. The dye/micropollutant removal efficiency of nanoemulsions was significantly influenced by droplet size and viscosity. Therefore, our results were in good agreement with previously published data of indomethacin and Congo red [22,25].

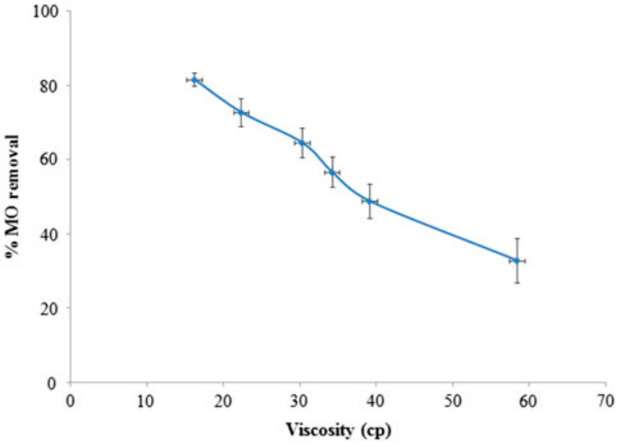

Fig. 3. Impact of viscosity of EA/Triton-X100/EG/water nanoemulsions on % MO removal ($n = 3$).

## 4. Conclusions

In the present study, attempts were made to develop EA/Triton-X100/EG/water nanoemulsions for the removal of MO from aqueous solution. Developed nanoemulsions passed thermodynamic stability and self-nanoemulsification tests. The droplet size, viscosity, and % removal of MO by EA/Triton-X100/EG/water nanoemulsions were significantly influenced by oil phase concentration. However, contact time had negligible influence on MO removal. Based on lowest droplet size (18.6 nm), lowest viscosity (16.2 cp) and highest % MO removal efficiency (81.6%), the nanoemulsion $G_1$ (containing 5% w/w of EA, 23.3% w/w of Triton-X100, 11.7% w/w of EG, and 60% w/w of water) was optimized as the best formulation for the removal of MO from aqueous solution after 20 min of contact time. The results of this study indicated that developed EA/Triton-X100/EG/water nanoemulsions could be a potential liquid-based system for the removal of MO orange from aqueous solution.

## Conflict of interest

The authors report no conflict of interest related with this manuscript.

## Acknowledgment

The authors would like to extend their sincere appreciation to the Deanship of Scientific Research at King Saud University for funding this research group No. RG 1435-005.

## References

[1] G. Crini, Non-conventional low-cost adsorbents for dye removal: A review, Bioresour. Technol. 97 (2006) 1061–1085.

[2] S. Chatterjee, D.S. Lee, M.W. Lee, S.H. Woo, Enhanced adsorption of Congo red from aqueous solutions by chitosan hydrogel beads impregnated with cetyl trimethyl ammonium bromide, Bioresour. Technol. 100 (2009) 2803–2809.

[3] S. Dawood, T.K. Sen, Removal of anionic dye congo red from aqueous solution by raw pine and acid-treated pine cone powder as adsorbent: Equilibrium, thermodynamic, kinetics, mechanism and process design, Water Res. 46 (2012) 1933–1946.

[4] J. Hastie, D. Bejan, M. Teutli-León, N. Bunce, Electrochemical methods for degradation of orange II (sodium 4-(2-hydroxy-1-naphthylazo) benzenesulfonate), Ind. Eng. Chem. Res. 45 (2006) 4898–4904.

[5] S. Chen, J. Zhang, C. Zhang, Q. Yue, Y. Li, C. Li, Equilibrium and kinetic studies of methyl orange and methyl violet adsorption on activated carbon derived from *Phragmites australis*, Desalination 252 (2010) 149–156.

[6] F. Shakeel, N. Haq, F.K. Alanazi, I.A. Alsarra, Box–Behnken statistical design for removal of methylene blue from aqueous solution using sodium dodecyl sulfate self-microemulsifying systems, Ind. Eng. Chem. Res. 53 (2014) 1179–1188.

[7] E. Haque, J.E. Lee, I.T. Jang, Y.K. Hwang, J.S. Chang, J. Jegal, S.H. Jhung, Adsorptive removal of methyl orange from aqueous solution with metal-organic frameworks, porous chromium-benzenedicarboxylates, J. Hazard. Mater. 181 (2010) 535–542.

[8] A. Mittal, A. Malviya, D. Kaur, J. Mittal, L. Kurup, Studies on the adsorption kinetics and isotherms for the removal and recovery of methyl orange from wastewaters using waste materials, J. Hazard. Mater. 148 (2007) 229–240.

[9] Z. Yao, L. Wang, J. Qi, Biosorption of methylene blue from aqueous solution using a bioenergy forest waste: *Xanthoceras sorbifolia* seed coat, Clean 37 (2009) 642–648.

[10] A. Mittal, V. Thakur, V. Gajbe, Evaluation of adsorption characteristics of an anionic azo dye Brilliant Yellow onto hen feathers in aqueous solutions, Environ. Sci. Pollut. Res. 19 (2012) 2438–2447.

[11] V.K. Gupta, D. Pathania, S. Agarwal, S. Sharma, Removal of Cr(VI) onto *Ficus carica* biosorbent from water, Environ. Sci. Pollut. Res. 20 (2013) 2632–2644.

[12] T.K. Sen, S. Afroze, H.M. Ang, Equilibrium, kinetics and mechanism of removal of methylene blue from aqueous solution by adsorption onto pine cone biomass of *Pinus radiata*, Water Air Soil Pollut. 218 (2011) 499–515.

[13] P.M.K. Reddy, S.K. Mahammadunnisa, B. Ramaraju, B. Sreedhar, C.H. Subrahmanyam, Low cost adsorbents from bio-waste for the removal of dyes from aqueous solution, Environ. Sci. Pollut. Res. 20 (2013) 4111–4124.

[14] M.A. Rauf, I. Shehadeh, A. Ahmed, A. Al-Zamly, Removal of methylene blue from aqueous solution by using gypsum as a low cost adsorbent, World Acad. Sci. Eng. Technol. 31 (2009) 604–609.

[15] M. Ghaedi, A. Hassanzadeh, N.S. Kokhdan, Multiwalled carbon nanotubes as adsorbents for the kinetic and equilibrium study of the removal of alizarin red S and Morin, J. Chem. Eng. Data 56 (2011) 2511–2520.

[16] I. Mohmood, C.B. Lopes, I. Lopes, I. Ahmad, A.C. Duarte, E. Pereira, Nanoscale materials and their use in water contaminants removal: A review, Environ. Sci. Pollut. Res. 20 (2013) 1239–1260.

[17] S. Shafiq, F. Shakeel, S. Talegaonkar, F.J. Ahmad, R.K. Khar, M. Ali, Development and bioavailability assessment of ramipril nanoemulsion formulation, Eur. J. Pharm. Biopharm. 66 (2007) 227–243.

[18] F. Shakeel, N. Haq, M. El-Badry, F.K. Alanazi, I.A. Alsarra, Ultra fine super self-nanoemulsifying drug delivery system (SNEDDS) enhanced solubility and dissolution of indomethacin, J. Mol. Liq. 180 (2013) 89–94.

[19] F. Shakeel, N. Haq, F.K. Alanazi, I.A. Alsarra, Impact of various nonionic surfactants on self-nanoemulsification efficiency of two grades of Capryol (Capryol-90 and Capryol-PGMC), J. Mol. Liq. 182 (2013) 57–63.

[20] F. Shakeel, N. Haq, F.K. Alanazi, I.A. Alsarra, Removal of xylenol orange from its aqueous solution using SDS-self-microemulsifying systems: Optimization by Box–Behnken statistical design, Environ. Sci. Pollut. Res. 21 (2014) 5187–5200.

[21] F. Shakeel, N. Haq, F.K. Alanazi, I.A. Alsarra, Development of dilutable green nanoemulsions for removal of Eriochrome black T from aqueous solution and optimization by Box–Behnken design, J. Mol. Liq. 196 (2014) 340–347.

[22] N. Haq, F.K. Alanazi, I.A. Alsarra, F. Shakeel, Potential of green nanoemulsions in removal of Congo red from aqueous solution, Sep. Sci. Technol. 49 (2014) 2568–2573, doi: 10.1080/01496395.2014.928893.

[23] T.N.C. Dantas, K.R. Oliveira, A.A.D. Neto, M.C.P.A. Moura, The use of microemulsions to remove chromium from industrial sludge, Water Res. 43 (2009) 1464–1470.

[24] G. Song, S.X. Hai, C.Q. De, G.H. Cheng, Solvent extraction of thorium (IV) using W/O microemulsions, Sci. Chin. Chem. 55 (2012) 1712–1718.

[25] F. Shakeel, N. Haq, T.S. Sumague, F.K. Alanazi, I.A. Alsarra, Removal of indomethacin from aqueous solution using multicomponent green nanoemulsions, J. Mol. Liq. 198 (2014) 329–333, doi: 10.1016/j.molliq.2014.07.026.

[26] C. Bilbao-Sáinz, R.J. Avena-Bustillos, D.F. Wood, T.G. Williams, T.H. McHugh, Nanoemulsions prepared by a low-energy emulsification method applied to edible films, J. Agric. Food. Chem. 58 (2010) 11932–11938.

[27] F. Shakeel, S. Shafiq, N. Haq, F.K. Alanazi, I.A. Alsarra, Nanoemulsions as potential vehicles for transdermal and dermal delivery of hydrophobic compounds: An overview, Expert Opin. Drug Delivery 9 (2012) 953–974.